Available online at www.sciencedirect.com
SCIENCE DIRECT
Quaternary Research 66 (2006) 119–132
QUATERNARY RESEARCH
www.elsevier.com/locate/yqres

Late Quaternary paleosols, stratigraphy and landscape evolution in the Northern Pampa, Argentina

Rob A. Kemp [a,*], Marcelo Zárate [b], Phillip Toms [c], Matthew King [a], Jorge Sanabria [d], Graciella Arguello [d]

[a] *Department of Geography, Royal Holloway, University of London, Egham, Surrey TW20 0EX, UK*
[b] *CONICET and Universidad Nacional de la Pampa, Santa Rosa, Argentina*
[c] *School of Environment, University of Gloucestershire, Cheltenham, Gloucestershire GL50 4AZ, UK*
[d] *Facultad de Ciencias Exactas y Naturales, Universidad Nacional de Córdoba, Argentina*

Received 21 March 2005
Available online 14 February 2006

Abstract

The field properties, micromorphology, grain-size, geochemistry, and optically stimulated luminescence (OSL) ages of two late Quaternary sections have been used to reconstruct the sequence of pedosedimentary processes and to provide insights into landscape evolution in part of the Northern Pampa of Argentina. Paleosols developed in paludal sediments adjacent to the Paraná river at Baradero and in loess at Lozada can both be correlated and linked to other sites, thus enabling for the first time the tentative recognition and tracing of a diachronous soil stratigraphic unit that probably spans the equivalent of at least part of marine oxygen isotope stage (OIS) 5. The paleosol at Lozada was truncated and buried beneath fluvial sediments during the time span of OIS 4 and 3. Eolian gradually replaced paludal inputs at Baradero over this period, and there were also two clearly defined breaks in sedimentation and development of paleosols. The period corresponding to OIS 2 was marked by significant loess accumulation at both sites with accretion continuing into the mid-Holocene only at Lozada. The more developed nature of the surface soil at Baradero probably reflects a combination of a moister climate and a longer soil-forming interval.

Keywords: Paleosols; Loess; Argentina; Pedosedimentary processes; Micromorphology; OSL dating; Soil stratigraphy

Introduction

Loess–paleosol sequences in North America, Europe and China have frequently been used to reconstruct the pedosedimentary evolution of landscapes (e.g., McDonald and Busacca, 1990; Mestdagh et al., 1999; Kemp et al., 2001) and to provide regional to global proxy records of climatic change (e.g., Antoine et al., 2001; Kemp, 2001; Muhs et al., 2003). Studies of such sequences in the Southern Hemisphere, including the well known and extensive loess region of Argentina (Fig. 1), have yet to make the same impact as their northern counterparts. Progress here has been hampered by the lack of a *widely recognized* loess–paleosol stratigraphy, limited chronological controls, and few detailed (micro)morphological and analytical characterizations of paleosols (Imbellone and Teruggi, 1993; Muhs and Zárate, 2001; Zárate, 2003).

A late Quaternary stratigraphic framework for part of the loess region centered on Santa Fé, Entre Rios and Córdoba provinces (Fig. 1) has been established by Iriondo (1997, 1999), Kröhling (1999a,b) and Carignano (1999). Although paleosols were recognized at some sites within and beneath the main loess unit, the Tezanos Pinto Formation, no formal soil stratigraphic units were defined (Table 1a). The Tezanos Pinto Formation is bracketed by thermoluminescence (TL) ages of ca. 36,000 and 8500 yr (Kröhling, 1999a), yet recent optically stimulated luminescence (OSL) ages obtained from the type-site at Tortugas, 100 km west of Rosario (Fig. 1) (Kemp et al., 2004a) suggest that the base of this unit may be considerably older (ca. 150,000 yr). Three paleosols were locally recognized and defined as geosols in the Río Cuarto area of southern Córdoba province (Fig. 1) by Cantú (1992). The youngest Las Tapias Geosol, developed in a loess mantle (La Invernada

* Corresponding author.
E-mail address: r.kemp@rhul.ac.uk (R.A. Kemp).

0033-5894/$ - see front matter © 2006 University of Washington. All rights reserved.
doi:10.1016/j.yqres.2006.01.001

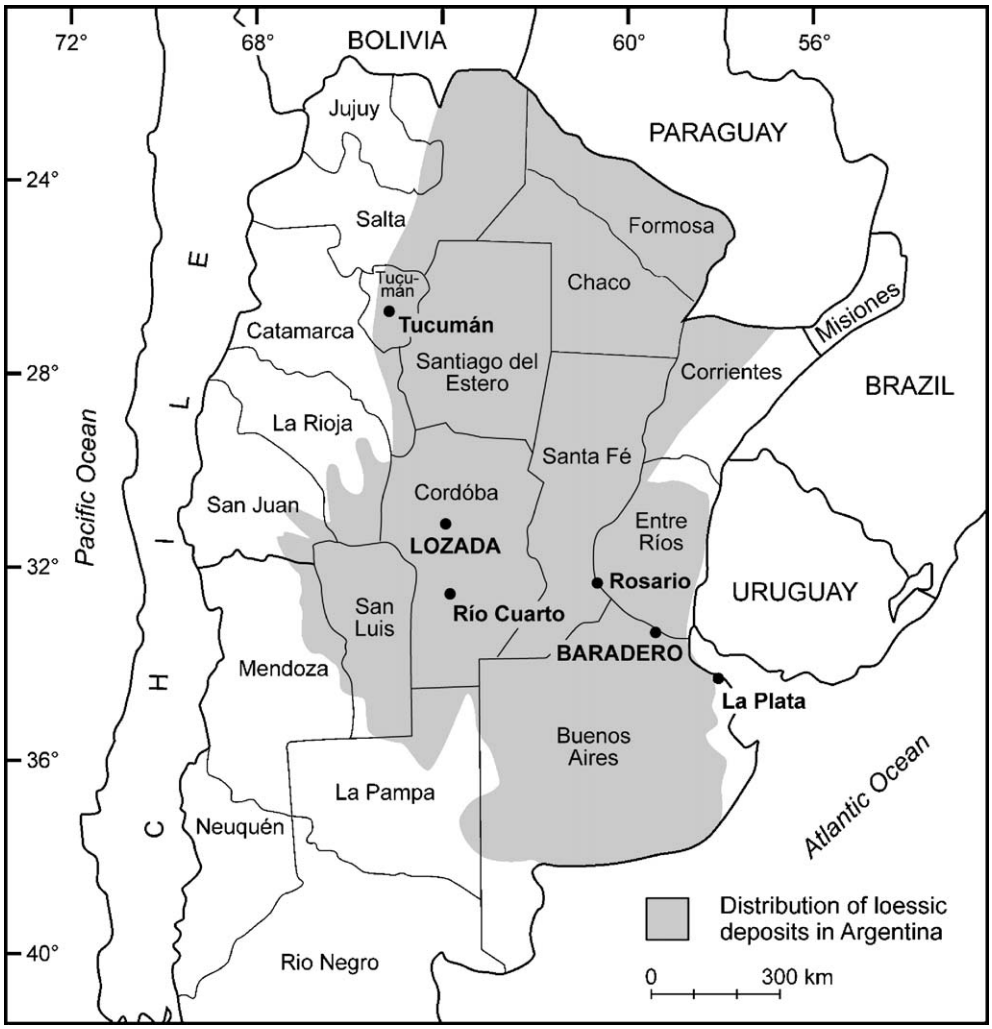

Figure 1. Distribution of loessic sediments in Argentina (after Zinck and Sayago, 1999; Zárate, 2003) and location of provinces, cities and study sites (Lozada and Baradero) referred to in the text.

Formation), is stratigraphically equivalent to the Hypsithermal soil of Kröhling (1999a). The older La Colacha and Estancia Cerrito Geosols are formed in late Pleistocene fluvial and Mid to Late Pleistocene eolian sediments, respectively (Cantú, 1992). A number of paleosols have been identified in northern Buenos Aires Province (Fig. 1) (e.g., Imbellone and Cumba, 2003; Imbellone and Teruggi, 1993; Tonni et al., 1999), though it has not been possible to correlate them with the sequences further north. Table 1b summarizes the general stratigraphy

Table 1a
Late Quaternary stratigraphy in Santa Fé and Córdoba provinces, the chronology based on a combination of thermoluminescence and calibrated radiocarbon age estimates (after Kröhling, 1999a)

Unit	Environment	Age/yr
Surface soil	Warm and humid	1400–
San Guillermo Fm	Semiarid	3500–1400
Hypsithermal soil	Warm and humid	8500–3500
Tezanos Pinto Fm	Semiarid	14,000–8500
Ck horizon	Semiarid/subhumid	16,000–14,000
Tezanos Pinto Fm	Arid	36,000–16,000
Paleosol	Warm and humid	65,000–36,000
Carcaraña Fm	Semiarid	
Paleosol	Warm and humid	
Pampean sand sea	Cold desert	

Table 1b
Quaternary stratigraphy in Buenos Aires province (after Riggi et al., 1986; Tonni et al., 1999)

Unit	Environment	Paleomagnetic chron and age
Surface soil	Warm and humid	Brunhes, <780,000 yr
Buenos Aires Fm: I	Semiarid to arid	
Paleosol	Warm and humid	
Buenos Aires Fm: II	Semiarid	
Paleosol	Warm and humid	
Buenos Aires Fm: III	Semiarid	
El Tala Geosol	Warm and humid	
Ensenada Fm	Semiarid	
Hisisa Geosol	Warm and humid	Matuyama, >780,000 yr
Ensenada Fm	Semiarid	
Paleosol	Warm and humid	
Ensenada Fm	Semiarid	
Paleosol	Warm and humid	
Ensenada Fm	Semiarid	

around La Plata (Fig. 1), the only chronological control being provided by the presence of the Brunhes–Matuyama magnetic boundary at the top of the Hisisa Geosol (Tonni et al., 1999).

Twenty-eight paleosols have been recognized and described in one 40-m section by Zinck and Sayago (1999, 2001) at La Mesada near Tafi-del-Valle, ca. 50 km west of San Miguel de Tucumán in northwest Argentina (Fig. 1). On the basis of four radiocarbon ages derived from the alkali-extract fractions of organic material, they proposed that most of the loess accumulated between ca. 17,500 and 27,500 ^{14}C yr B.P. This chronology was subsequently brought into question by three OSL age estimates, ranging from ca. 150,000 to 195,000 yr, obtained from the lowermost part of this section (Kemp et al., 2003) and the publication of paleomagnetic data from a different exposure in the Tafí-del-Valle region that indicates a basal age of at least 1.15 million yr (Schellenberger et al., 2003). Minimum OSL estimates of 165,000 yr from the base of another section at El Lambedero, 12 km north-east of La Mesada, reaffirmed the apparent antiquity of the Tafi sequences, though failed to enable the correlation of paleosol or loess units between the sites (Kemp et al., 2004b).

Tortugas and El Lambedero are sites that we have studied (Kemp et al., 2004a,b) as part of a regional project aimed at providing a more refined chronological and pedostratigraphic framework for the Argentinian loess region. In this paper we present the results from two other sites along the southeast–northwest transect, Lozada in Córdoba province and Baradero in Buenos Aires province (Fig. 1), that build upon our earlier work and enable the reconstruction, dating and correlation of late Quaternary pedosedimentary processes and landscape evolution.

Study sites and methodology

Lozada

The 9.3-m vertical section at Lozada (Fig. 1: 31° 39′S; 64° 08′W; 490 m a.s.l.) is exposed along an abandoned road excavation on an extensive plain, 35 km south of Córdoba city, within a geomorphological association mapped as 'alluvial paleofans with loess cover' by Sanabria and Arguello (1999). The region currently has a mean annual precipitation (MAP) of 700 mm, mainly concentrated during the summer, and a mean annual temperature (MAT) of 18°C (INTA, 1989). Sanabria and Arguello (1999) described the surficial soils in the area as Typic Haplustolls (Soil Survey Staff, 1992) developed in Holocene loess (TL ages of ca. 3000–6000 yr) with a grain size dominated by coarse silt. The main source area for the loess is the Andes Cordillera with a secondary contribution likely from the Sierras Pampeanas (Kröhling, 1999b), located 20 km to the west of the site.

Baradero

The exposure at Baradero (Fig. 1: 33° 47′S, 59° 39′W; 70 m a.s.l.), located 140 km northwest of Buenos Aires city, is a 17-m vertical cliff along the right margin, and 100 m away from one of the main channels of the Paraná river (Fig. 1). The region currently has a MAP of 900 mm and a MAT of 18°C: the dominant surface soil is a Typic Argiudoll (INTA, 1989; Soil Survey Staff, 1992). Previous work in the area by Nabel et al. (1993) identified a number of lithostratigraphic units that were broadly correlated with the regional stratigraphy (Table 1b). Their focus was on the magnetostratigraphy, the differentiation of the Ensenada and Buenos Aires Formations (Riggi et al., 1986) and the recognition of the El Tala and Hisisa Geosols. Possible paleosols in the upper 6–7 m of the exposure were not studied in any detail. Camilión et al. (1992) and Nabel et al. (1993), largely on the basis of particle size distribution and clay mineral assemblages, suggested that a significant proportion of the sediments at Baradero have a 'paludal' (flood basin; Reineck and Singh, 1980) rather than eolian origin.

Methods

The sections were described and soil horizons identified according to the criteria of the Soil Survey Staff (1992). Calcium carbonate and particle size analyses were undertaken on bulk samples at 5- or 10-cm vertical intervals using a calcimeter (Gale and Hoare, 1992) and a Malvern Laser Granulometer, respectively. The grain size results were expressed as median diameter (Md). Prior to particle size analyses, organic matter was removed using 30% hydrogen peroxide and sodium hexametaphosphate was added as a dispersant. Major element contents of bulk samples from 10- or 20-cm vertical intervals were determined following dissolution in perchloric, hydrofluoric and hydrochloric acids, and analysis on an Inductively Coupled Plasma-Atomic Emissions Spectrometer. From these data, variation of TiO_2/Na_2O weathering ratios (Grimley et al., 2003) with depth was plotted. Undisturbed blocks (7 × 5 × 4 cm) collected in Kubiena tins at approximately 25-cm vertical intervals were air-dried, impregnated with polyester resin and made into thin sections (7 × 5 cm) according to standard procedures (Lee and Kemp, 1992). The thin sections were described at 10–400× magnification under a petrological microscope using the terminology of Bullock et al. (1985), the estimated proportion of key micromorphological features being recorded as a function of depth.

Blocks of sediment (10 × 10 × 7.5 cm) were collected from 0.7, 1.4, 2.3, 3.6, 4.3, 5.5, 6.4, 8.0 and 9.0 m depths at Lozada and 0.4, 1.5, 2.6, 3.7 and 4.9 m depths at Baradero. Sediment ages were based on blue-green light stimulated OSL fine silt-sized quartz (Jackson et al., 1976; Berger et al., 1980). This time-dependent signal was calibrated using a single-aliquot regenerative-dose procedure to generate values of equivalent dose (D_e). Lithogenic dose rate was derived from elemental concentrations (Adamiec and Aitken, 1998) quantified through neutron activation analysis and in situ gamma spectroscopy. Appropriate corrections were made for moisture content (Zimmerman, 1971) and reduced sensitivity to α radiation. Calculation of cosmogenic dose rate followed the formulae of Prescott and Hutton (1994). Age is the quotient of the geometric mean D_e (central age model; Galbraith et al., 1999) and dose

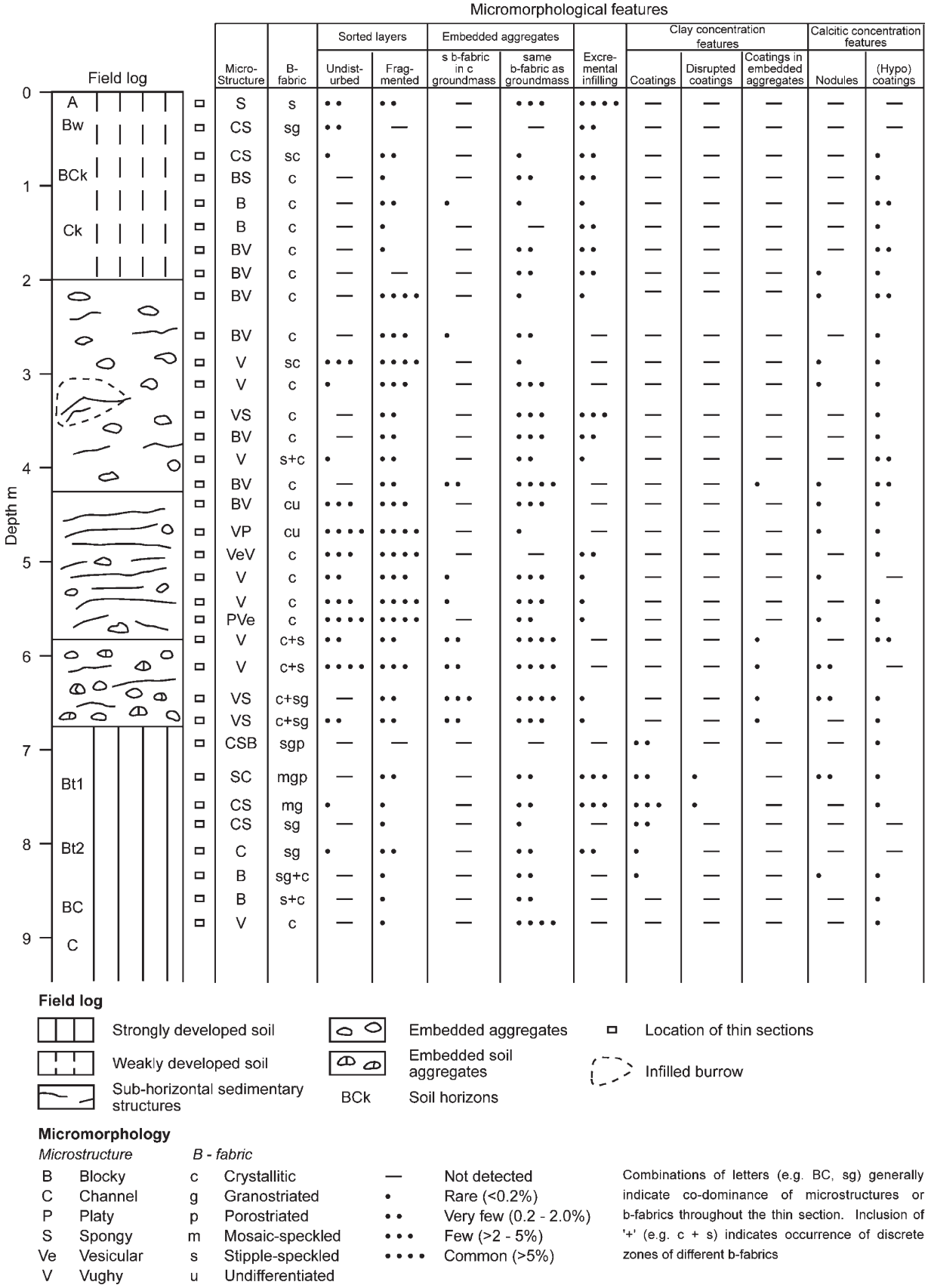

Figure 2. Field log and micromorphology of the profile at Lozada.

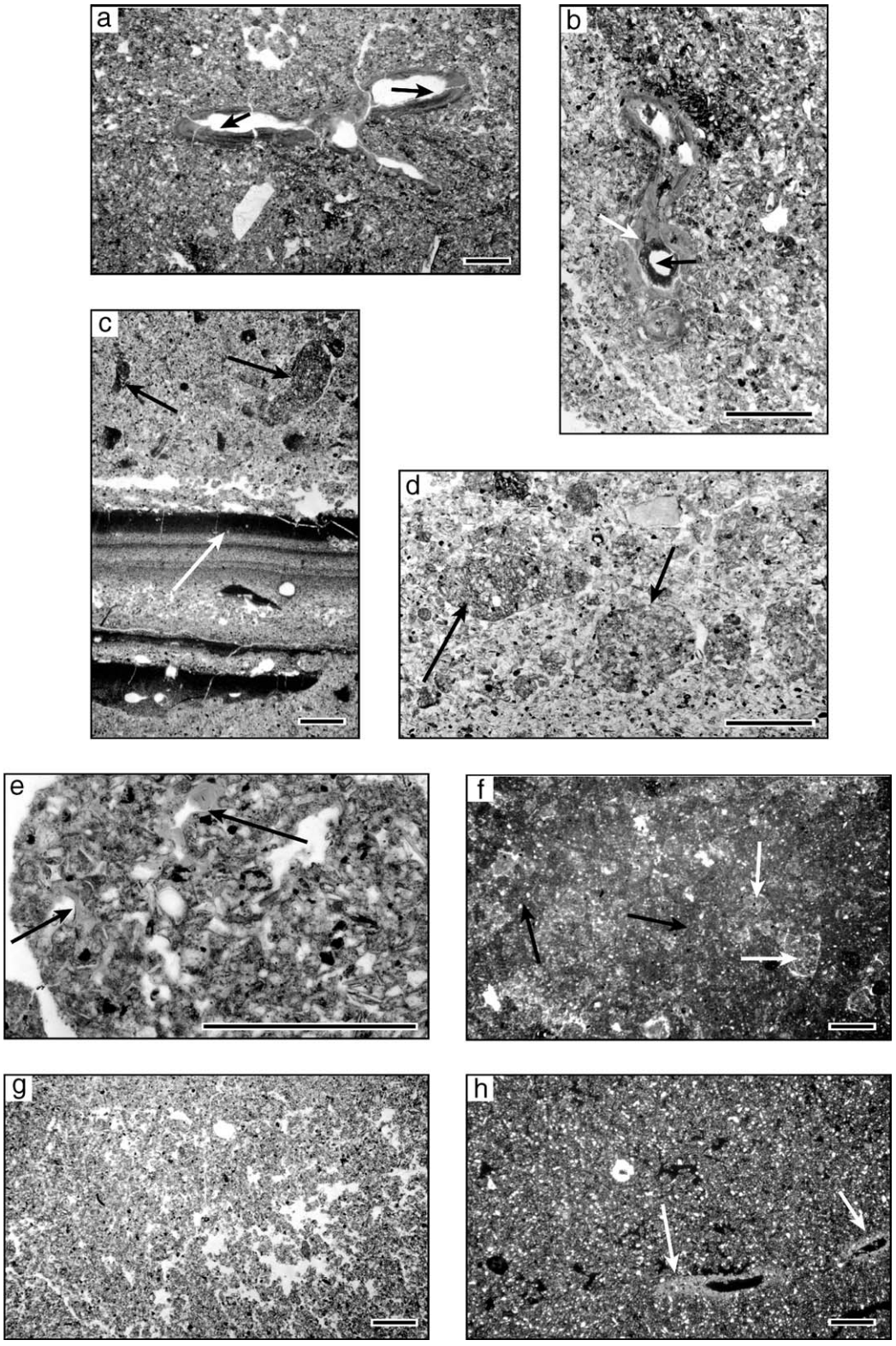

Figure 3. Photomicrographs of key micromorphological features from Lozada: plane polarized light (PPL); crossed polarized light (XPL); Scale bar = 600 μm. (a) Clay coatings (black arrows) around channels (7.5 m, PPL). (b) Calcitic coating (black arrow) covering (and therefore postdating) a clay coating (white arrow) around a channel (7.5 m, PPL). (c) Sorted layers (white arrow) and embedded aggregates (black arrows) (5.3 m, PPL). (d) Cluster of embedded aggregates (black arrows) (5.8 m, PPL). (e) Clay coatings (black arrows) within an embedded aggregate (6.5 m, PPL). (f) Aggregates with stipple-speckled b-fabric (white arrows) embedded within groundmass having crystallitic b-fabric (black arrows) (5.8 m, XPL). (g) Spongy microstructure (0.05 m, PPL). (h) Calcitic hypocoatings (white arrows) around channels (1.7 m, XPL).

rate values, and its error is based upon the propagation of systematic and experimental (1σ) uncertainties. Further details of the OSL dating methodology followed here is outlined in Toms et al. (2004).

Lozada

Field log and micromorphology

The Lozada profile comprises a surface soil and a basal truncated paleosol separated by over 4 m of sediment (Fig. 2). The paleosol has brown (7.5 YR 4/4) silty clay loam Bt and dark yellowish brown (10YR 4/4) silt loam BC and C horizons. Evidence of bioturbation and clay translocation processes is provided by the spongy or channel microstructures, excremental infillings and clay coatings (Fig. 3a) in the Bt horizons. Calcitic coatings covering, and therefore postdating, some of the clay coatings (Fig. 3b) suggest that the small amounts of secondary carbonate present as concentration features and patches of crystallitic b-fabric in the paleosol have resulted from post-burial precipitation of solutes leached down from the overlying sediments or present within groundwater.

Immediately above the sharp upper boundary of the Bt1 horizon and extending to the base of the present-day soil (6.7–2.0 m), the sediments are lighter (yellowish brown, 10YR 5/4) and texturally heterogeneous (silty clay loam, silt loam and fine sandy loam) with varying concentrations of continuous and discontinuous sub-horizontal laminations (<2 cm thick) that in thin sections are shown to comprise well-defined sorted layers of fine sand, coarse silt, fine silt and clay (Fig. 3c). At one location (3.2–3.4 m), these structures appear to be concentrated within an infilled megafaunal burrow suggesting sediment accumulation following subsurface flow. While clearly reflecting a degree of water sorting, however, some of these features elsewhere may have other origins including surface crusting or overland flow and sedimentation (Mücher and Vreeken, 1981; Kemp et al., 2004a). Once formed, they were subject to fragmentation and disruption, presumably either by erosion, desiccation or bioturbation processes.

Commonly, but not invariably, associated with the sorted structures are sub-rounded aggregates embedded within the groundmass and ranging in size from 1.5 cm to <0.2 mm (Figs. 3c and d). Some of these aggregates immediately above the truncated paleosol have undisturbed clay coatings around channels (Fig. 3e), suggesting that this zone contains reworked Bt and probably A/E horizon material that was derived from erosion of the paleosol from adjacent parts of the landscape. The few small embedded aggregates containing no illuvial clay features within the paleosol may date from an earlier phase of reworking, though these and some similar features above 5.8 m could have had faunal origins, particularly where they occur adjacent to well-defined excremental infillings.

Mobilization of calcium carbonate was probably another active process during the accumulation of the sediments

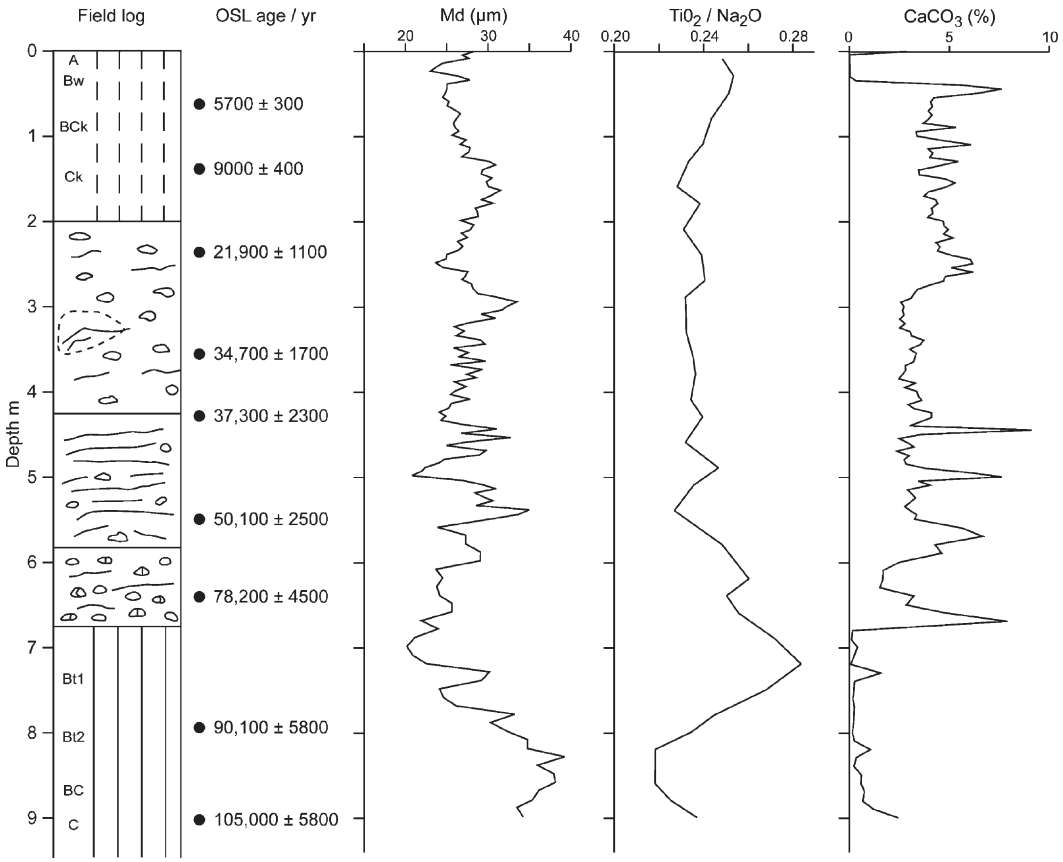

Figure 4. Field log and depth functions of OSL ages, Md, TiO_2/Na_2O and % $CaCO_3$ from the profile at Lozada.

overlying the truncated paleosol. The calcitic concentration features extending down into the paleosol and the micrite responsible for the ubiquitous crystallitic b-fabric formed by precipitation of solutes present within groundwater or leached down from accretionary surfaces. In places, as at Tortugas (Kemp et al., 2004a), the migrating solutes have been unable to infiltrate significantly into the interiors of the embedded aggregates and have thus 'fossilized' and emphasized the form of these stipple- or mosaic-speckled features (Fig. 3f).

The silt loam soil developed at the current surface has very dark grayish brown (10YR 3/2) A and dark yellowish brown (10YR 4/4) Bw horizons that are bioturbated with spongy microstructures (Fig. 3g) and leached with significant amounts of secondary carbonate accumulating lower down in the yellowish brown (10YR 5/4) BCk, and Ck horizons (Fig. 3h). Clay concentration features are absent throughout.

Bulk analysis and chronology

Figure 4 shows depth functions of Md, TiO_2/Na_2O ratio, % $CaCO_3$ plus a summary of the OSL age estimates for the Lozada profile. Full chronological data are provided in Table 2. The paleosol and surface soil have lowest Md values in their most illuviated and weathered horizons, respectively. Md throughout the profile predominantly ranges between 25 and 35 μm, reflective of the primary loessic origin of the sediments, though the identified phases of reworking and possible incorporation of other fluvial components have resulted in a variable depth distribution.

The TiO_2/Na_2O ratio, shown elsewhere to be a reliable indicator of weathering intensity particularly with regards Na-rich plagioclase feldspar (Muhs et al., 2001; Grimley et al., 2003), has maximum values in the A and Bw horizons of the surface soil and the Bt1 horizon of the paleosol. Even with its A and E horizons absent, the paleosol appears to be more weathered and developed than the surface soil, a notion reinforced by differences in field and micromorphological properties (e.g., illuvial clay coatings) also. The zone immediately above the truncated paleosol has relatively high ratios, presumably due to the previously-noted incorporation of eroded paleosol components from adjacent parts of the landscape. The vertical variation in calcium carbonate content is consistent with the morphological data, namely minor superimposition of secondary carbonate on the decalcified paleosol and development of a classic leaching profile in the surface soil. Carbonate content of the intervening sediments displays an irregular depth pattern, reflecting phases of syndepositional mobilization.

The OSL age estimates range from ca. 6000 to 105,000 yr and are in stratigraphic order throughout (Table 2 and Fig. 4). For all samples, infrared-stimulated luminescence following a laboratory dose similar in magnitude to D_e was insignificant, indicating limited contamination by feldspars (Fig. 5). Repeat regenerative-dose responses were statistically concordant. D_e values of 200–400 Gy, while large, fall within the functional range of dose responses (Fig. 5) and are consistent with those reported by Murray et al. (2002) for which the accuracy of associated OSL age estimates has

Table 2
Optical age estimates obtained from samples at Lozada (LOZ) and Baradero (BAR)

Site and depth (m)	Moisture content (fraction of wet weight)	NaI γ-spectrometry (in situ)			Total γ dose rate ($Gy.10^{-3}$ yr)	Neutron activation analysis			Total α dose rate ($Gy.10^{-3}$ yr)	Total β dose rate ($Gy.10^{-3}$ yr)	Cosmic dose rate ($Gy.10^{-3}$ yr)	Total dose rate ($Gy.10^{-3}$ yr)	Geometric mean D_e (Gy)	Geometric mean age (yr)
		K (%)	Th (ppm)	U (ppm)		K (%)	Th (ppm)	U (ppm)						
LOZ 0.7	0.13 ± 0.03	1.67 ± 0.01	8.94 ± 0.15	2.28 ± 0.06	1.09 ± 0.01	2.23 ± 0.11	12.30 ± 0.62	2.17 ± 0.11	0.50 ± 0.04	2.03 ± 0.13	0.20 ± 0.02	3.82 ± 0.14	21.7 ± 1.1	5700 ± 300
LOZ 1.4	0.09 ± 0.02	1.94 ± 0.02	9.48 ± 0.18	2.53 ± 0.08	1.21 ± 0.01	2.25 ± 0.11	11.90 ± 0.60	2.36 ± 0.12	0.54 ± 0.03	2.15 ± 0.12	0.18 ± 0.02	4.08 ± 0.12	36.6 ± 1.4	9000 ± 400
LOZ 2.3	0.09 ± 0.02	1.87 ± 0.03	9.30 ± 0.29	2.55 ± 0.13	1.18 ± 0.02	2.63 ± 0.13	11.10 ± 0.56	2.81 ± 0.14	0.56 ± 0.03	2.46 ± 0.14	0.15 ± 0.01	4.36 ± 0.14	95.4 ± 3.6	21,900 ± 1100
LOZ 3.6	0.08 ± 0.02	1.91 ± 0.02	9.70 ± 0.20	2.64 ± 0.09	1.22 ± 0.01	2.31 ± 0.12	12.00 ± 0.60	2.55 ± 0.13	0.57 ± 0.03	2.26 ± 0.12	0.12 ± 0.01	4.18 ± 4.51	144.8 ± 5.9	34,700 ± 1700
LOZ 4.3	0.04 ± 0.01	1.94 ± 0.03	10.20 ± 0.30	2.51 ± 0.13	1.24 ± 0.02	2.05 ± 0.21	12.10 ± 1.21	2.64 ± 0.26	0.65 ± 0.05	2.21 ± 0.16	0.10 ± 0.01	4.20 ± 0.17	156.7 ± 7.5	37,300 ± 2300
LOZ 5.5	0.09 ± 0.02	1.95 ± 0.02	9.82 ± 0.19	2.93 ± 0.09	1.27 ± 0.01	2.48 ± 0.12	13.30 ± 0.67	3.21 ± 0.16	0.66 ± 0.04	2.48 ± 0.13	0.09 ± 0.01	4.51 ± 0.14	226.2 ± 9.1	50,100 ± 2500
LOZ 6.4	0.13 ± 0.03	1.79 ± 0.03	9.30 ± 0.28	2.21 ± 0.12	1.13 ± 0.02	2.32 ± 0.12	13.10 ± 0.66	2.89 ± 0.14	0.59 ± 0.04	2.19 ± 0.14	0.08 ± 0.01	3.99 ± 0.15	312.1 ± 13.5	78,200 ± 4500
LOZ 8.0	0.13 ± 0.03	1.72 ± 0.02	9.23 ± 0.25	2.42 ± 0.11	1.13 ± 0.02	2.01 ± 0.20	12.10 ± 1.21	2.36 ± 0.24	0.44 ± 0.04	1.89 ± 0.16	0.06 ± 0.01	3.53 ± 0.17	317.9 ± 13.6	90,100 ± 5800
LOZ 9.0	0.12 ± 0.03	1.90 ± 0.02	9.11 ± 0.18	2.24 ± 0.08	1.15 ± 0.01	2.39 ± 0.12	12.00 ± 0.60	2.28 ± 0.11	0.51 ± 0.04	2.17 ± 0.14	0.06 ± 0.01	3.90 ± 0.14	409.1 ± 17.3	105,000 ± 5800
BAR 0.4	0.11 ± 0.03	1.42 ± 0.02	8.58 ± 0.19	1.99 ± 0.08	0.98 ± 0.01	1.92 ± 0.10	11.70 ± 0.59	1.77 ± 0.09	0.46 ± 0.03	1.79 ± 0.11	0.14 ± 0.01	3.37 ± 0.12	48.4 ± 2.0	14,400 ± 800
BAR 1.5	0.05 ± 0.01	1.59 ± 0.02	10.09 ± 0.17	2.23 ± 0.07	1.12 ± 0.01	1.74 ± 0.17	12.90 ± 1.29	1.90 ± 0.19	0.47 ± 0.04	1.88 ± 0.14	0.16 ± 0.03	3.62 ± 0.15	100.6 ± 3.6	27,800 ± 1500
BAR 2.6	0.12 ± 0.03	1.42 ± 0.02	9.25 ± 0.22	1.97 ± 0.09	1.01 ± 0.02	1.75 ± 0.09	12.20 ± 0.61	1.82 ± 0.09	0.48 ± 0.03	1.69 ± 0.11	0.20 ± 0.03	3.36 ± 0.12	185.8 ± 7.2	55,200 ± 2900
BAR 3.7	0.15 ± 0.04	1.41 ± 0.02	9.21 ± 0.18	1.65 ± 0.07	0.97 ± 0.01	1.82 ± 0.09	12.20 ± 0.61	1.63 ± 0.08	0.43 ± 0.04	1.63 ± 0.12	0.12 ± 0.01	3.14 ± 0.13	245.1 ± 9.4	77,900 ± 4400
BAR 4.9	0.16 ± 0.04	1.39 ± 0.02	8.61 ± 0.22	1.80 ± 0.09	0.95 ± 0.02	1.82 ± 0.09	11.30 ± 0.57	1.58 ± 0.08	0.40 ± 0.03	1.59 ± 0.12	0.10 ± 0.01	3.04 ± 0.13	347.1 ± 16.2	114,300 ± 7200

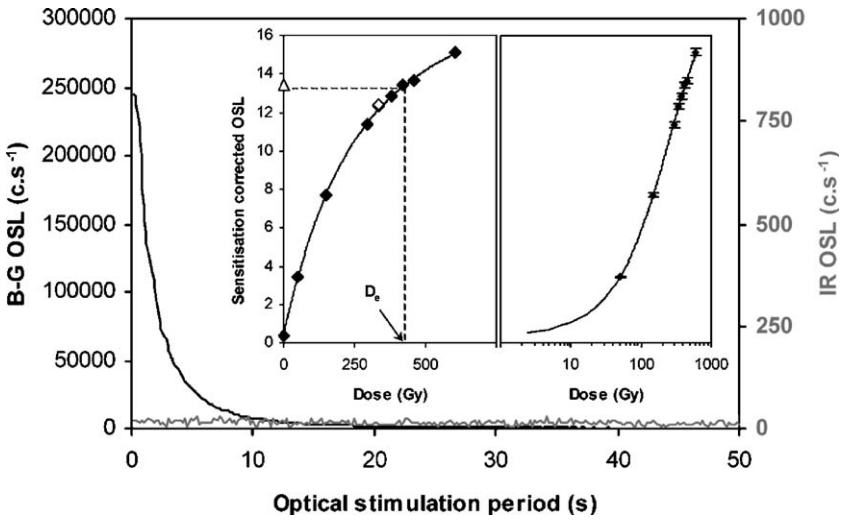

Figure 5. Blue-green and infrared natural OSL for a fine silt-sized quartz aliquot of LOZ 9.0 (m). Inset left: dose response and interpolated D_e value for the same aliquot showing the natural and repeat regenerative-dose signals (open triangle and open diamond, respectively). Inset right: dose response fitted with a single exponential and the functional (non-saturated) dose range is evidenced in the log-linear plot by the statistically significant increase in dose response beyond the point of interpolation (Murray and Funder, 2003).

been verified. The interpretation of luminescence ages from pedogenically altered sediments, however, is not necessarily straightforward. The apparent age of parent material may be modulated by pedoturbation of the minerogenic dosimeter (quartz) and pedogenically induced matrix variations in radionuclide composition (Singhvi et al., 2001; Bateman et al., 2003; Berger, 2003; Goble et al., 2004). Further complications may arise where older material occurs within transported aggregates, as here, potentially affecting the bulk luminescence characteristics of a horizon. Sub-aqueous erosion, transport and deposition of components at Lozada may also promote age overestimation through partial bleaching of the chronometric signal, though the significance of this effect is probably limited given the relatively large dose exposure of each sample (Olley et al., 2004). Notwithstanding all these caveats, it is reasonable to suggest from the data that the paleosol formed at some period between ca. 105,000 (or possibly 90,000) and 80,000 yr. OSL ages of 9000 ± 400 and 5700 ± 300 yr at 1.5 m and 0.5 m, respectively, demonstrate that significant quantities of loess likely accumulated in this region at least until after the mid-Holocene, thus perhaps providing a reason for the relatively weak development of the surface soil.

Baradero

Field log and micromorphology

The field log and micromorphology of the Baradero profile are summarized in Figure 6. A major boundary occurs at approximately 3.1 m where there is a marked transition from predominantly strong brown (7.5YR 4/6) silty clay to overlying brownish yellow (10YR 6/6) silty clay loam. The basal fine-textured unit contains variable quantities of clay coatings and secondary carbonate features that enable differentiation into Bt, Btk and BCk horizons, any A and/or E horizon apparently having been eroded or reworked and incorporated within covering sediments. The zone above the uppermost Bt horizon, between 3.8 and 3.1 m, is dominated by the presence of a dense network of strong brown (7.5YR 4/6) prismatic or subangular blocky (<4 cm) and cylindrical (<15 × 1 cm) aggregates of silty clay separated by brownish yellow (10YR 6/6) silty clay loam. The relative proportion of these aggregates gradually declines above this zone until, at ca. 1.3 m, the matrix is entirely composed of yellowish brown (10YR 5/8) silty clay loam. At the micromorphological scale, there are also a few embedded aggregates and sorted layer features similar to those described from Lozada.

This vertical change in lithology at Baradero is a reflection of two very different sedimentary regimes. Initially, the site was subjected to periodic flooding and deposition of fine-grained suspended load. Bioturbation was probably active as the silty clay paludal deposits accreted within a swampy environment, though the paleosol itself presumably marks a depositional hiatus and establishment of a relatively stable land surface at which other pedogenic processes of leaching and clay translocation became significant. In fact, the paleosol horizon sequence and depth distribution of key micromorphological features [calcitic concentrations, undisturbed and fragmented clay coatings (Figs. 7a and b), sorted layers and embedded aggregates] suggest a complex pedosedimentary history for this unit, perhaps involving cycles of deposition, pedogenesis and reworking with two, or possibly three, truncated paleosols welded to each other (>5.2 m, 4.4–5.2 m and 3.8–4.6 m).

Between 3.8 and 1.3 m marks a transitional period with increasing dominance of eolian inputs to the site. Some of silty clay loam loess initially appears to have accumulated within desiccation fissures separating blocky and prismatic aggregates of the silty clay paludal sediments, though the prevalence of cylindrical aggregates (excremental infillings in thin sections) and spongy microstructures (Fig. 7c) support the notion that bioturbation processes were primarily responsible for mixing the two materials. Other pedogenic processes, notably leaching and clay translocation, were clearly active at stages during this

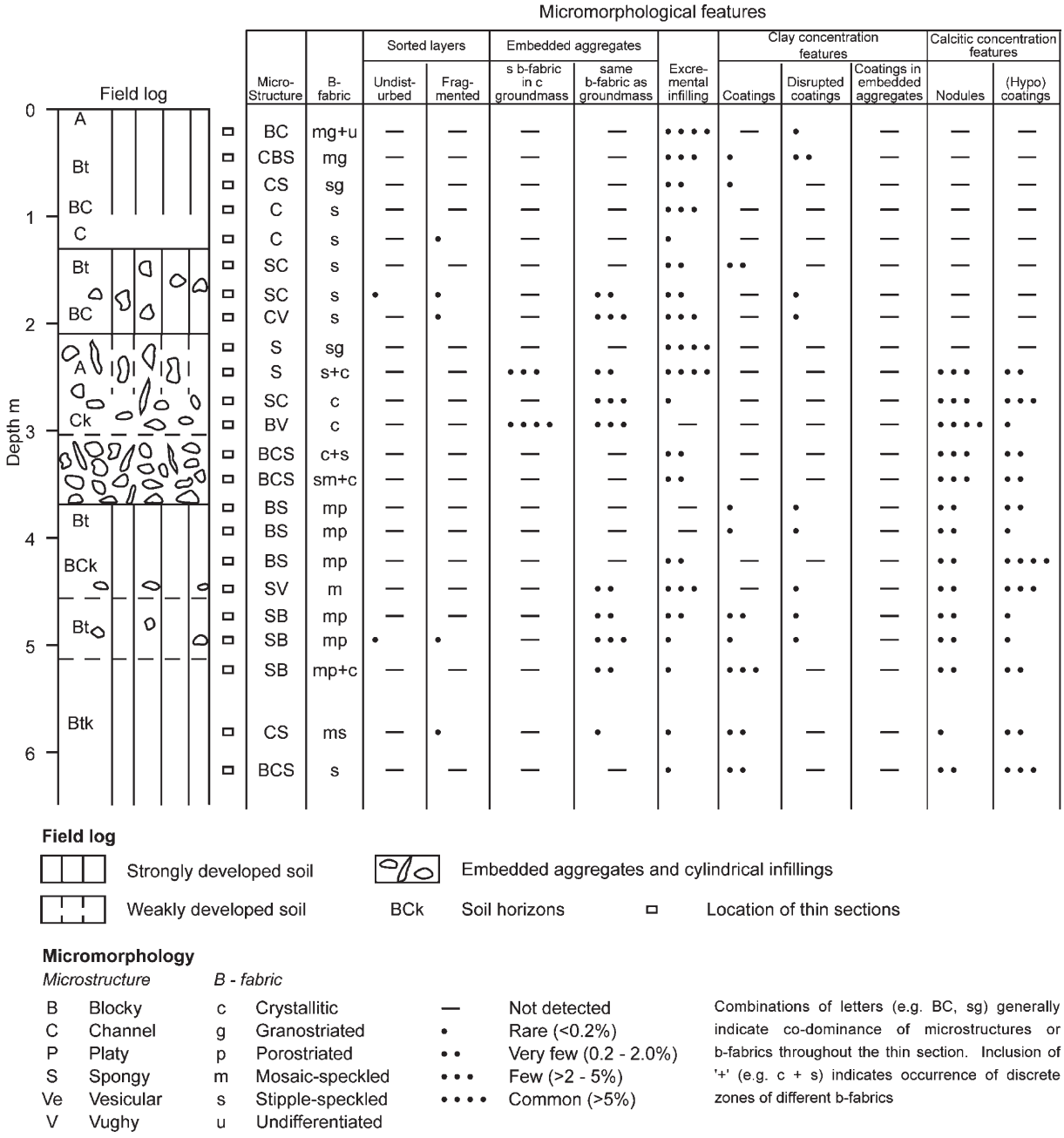

Figure 6. Field log and micromorphology of the profile at Baradero.

period, as evidenced by the presence of clay coatings and calcitic concentration features (Fig. 7d). Two abutting paleosols can be demarcated; a lower A/Ck profile overlain by a more strongly developed Bt/BC/C profile that is morphologically similar to the soil developing in loess at the current surface. The A/E horizon of the uppermost paleosol is absent, either diagenetically-converted to the C horizon of the surface soil or, more likely in view of the relative dearth of bioturbation features at this level, eroded.

Bulk analysis and chronology

Figure 8 shows depth functions of Md, TiO_2/Na_2O ratio, % $CaCO_3$ plus a summary of the optical age estimates for the Baradero profile. Full chronological data are provided in Table 2. The paludal sediments in the lower half of the profile have Md values ranging between 5 and 10 μm. The texture coarsens above 3.1 m, reflecting the increasing proportions of wind-blown material, though it is finer throughout (Md is <25 μm) than the loess at Lozada.

The TiO_2/Na_2O weathering ratio curve has two distinct peaks in the upper 2.5 m that coincide with A horizons of the surface soil and a paleosol (2.2 m). A further minor peak is associated with the Bt horizon of the intervening paleosol (1.3 m), perhaps indirectly supporting the notion that its most weathered (A) horizon has been eroded. Conversely, the very high value immediately above the paleosol (complex) developed in paludal sediments (ca. 3 m) possibly reflects the

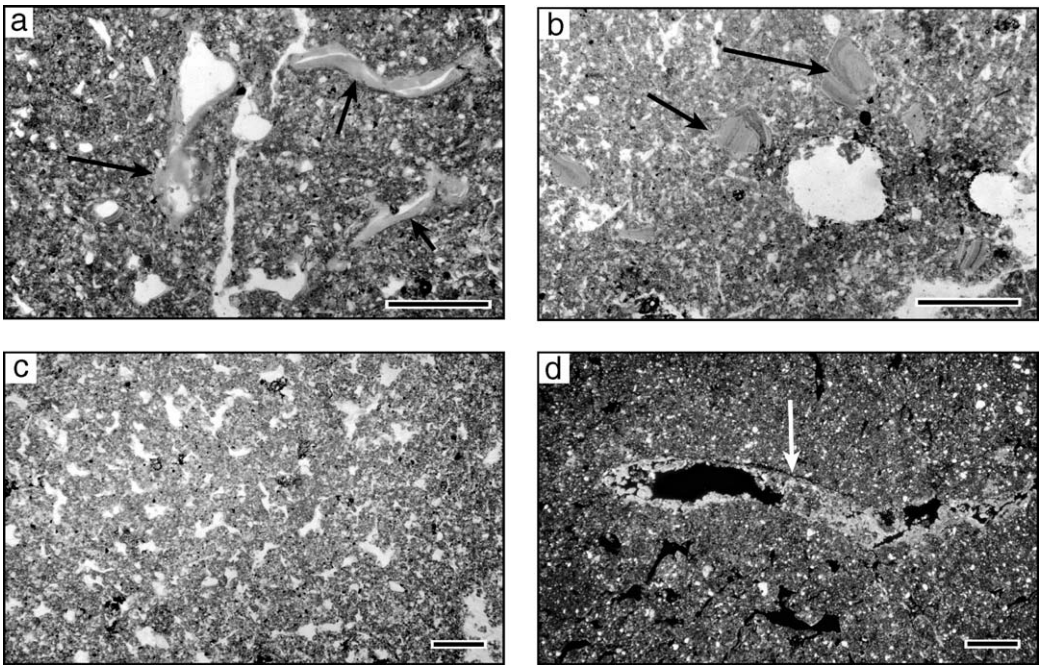

Figure 7. Photomicrographs of key micromorphological features from Baradero: plane polarized light (PPL); crossed polarized light (XPL); scale bar = 600 μm. (a) Clay coatings (black arrows) around channels (4.8 m, PPL). (b) Fragmented clay coatings (black arrows) embedded within groundmass (4.8 m, PPL), Spongy microstructure (2.2 m, PPL), Calcitic hypocoating (white arrow) around a channel (2.9 m, XPL).

presence of reworked A horizon material. Interpretation of the vertical trends in the weathering ratio, however, is complicated by the fact that the initial parent material composition was not uniform (Muhs et al., 2001) due to variable proportions of paludal and eolian inputs over time. The depth function of calcium carbonate content is consistent with the morphological data, namely strongly leached in the upper 2 m with a concentration of secondary carbonate in the Ck horizon of the second paleosol. Secondary carbonate has clearly also accumulated in the basal paleosol with the peak values in the BCk and underlying Btk horizons perhaps supporting the concept that this unit is a complex comprising several welded paleosols, though precipitation may alternatively be associated with post-burial groundwater oscillations.

The OSL ages of pedogenically-altered paludal and eolian sediments from Baradero range from ca. 14,000 to 114,000 yr and are in stratigraphic order (Table 2 and Fig. 8). They suggest that the basal paleosol complex probably dates back prior to ca.

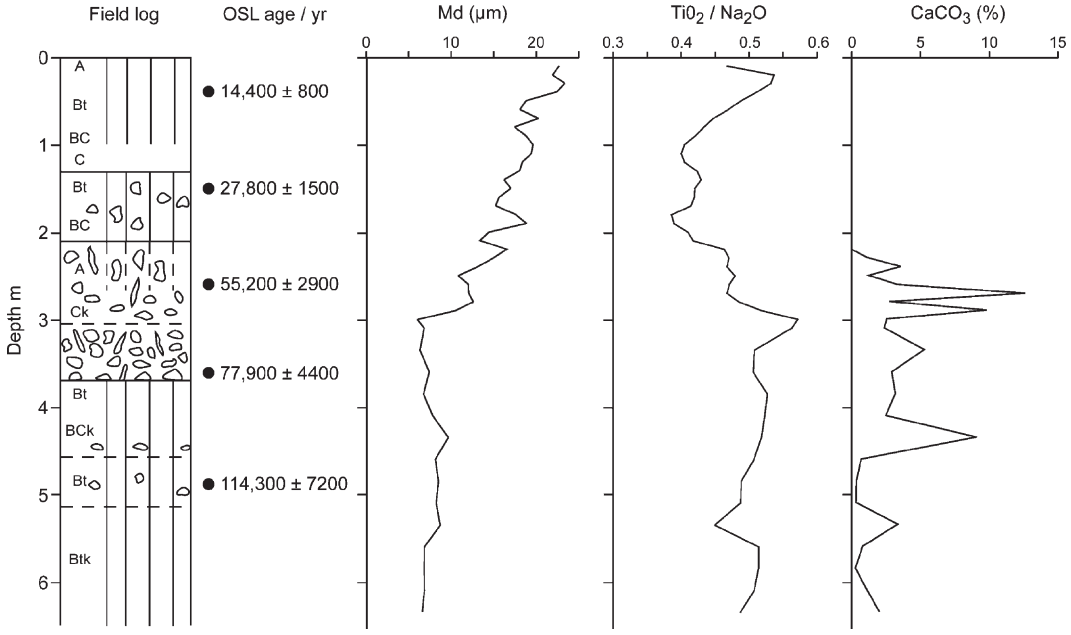

Figure 8. Field log and depth functions of OSL ages, Md, TiO_2/Na_2O and % $CaCO_3$ from the profile at Baradero.

80,000 yr, while the other two paleosols formed over some periods between ca. 80,000 and 25,000 yr. The surface soil, in contrast to Lozada, has developed largely in pre-Holocene loess.

Discussion

Figure 9 summarizes the sequence of pedosedimentary stages responsible for the formation of the sequences at Lozada and Baradero with OSL age estimates used to correlate activity between sites. Pedosedimentary stage 1 at Lozada involved a period of loess sedimentation, followed by establishment of a land surface and development of a soil with bioturbation, leaching and clay translocation processes prevalent. A similar sequence of events may have occurred at Baradero, though the soil parent material comprised fine-grained paludal sediments rather than loess. Furthermore, the pedosedimentary history here may be more complex with additional phase(s) of

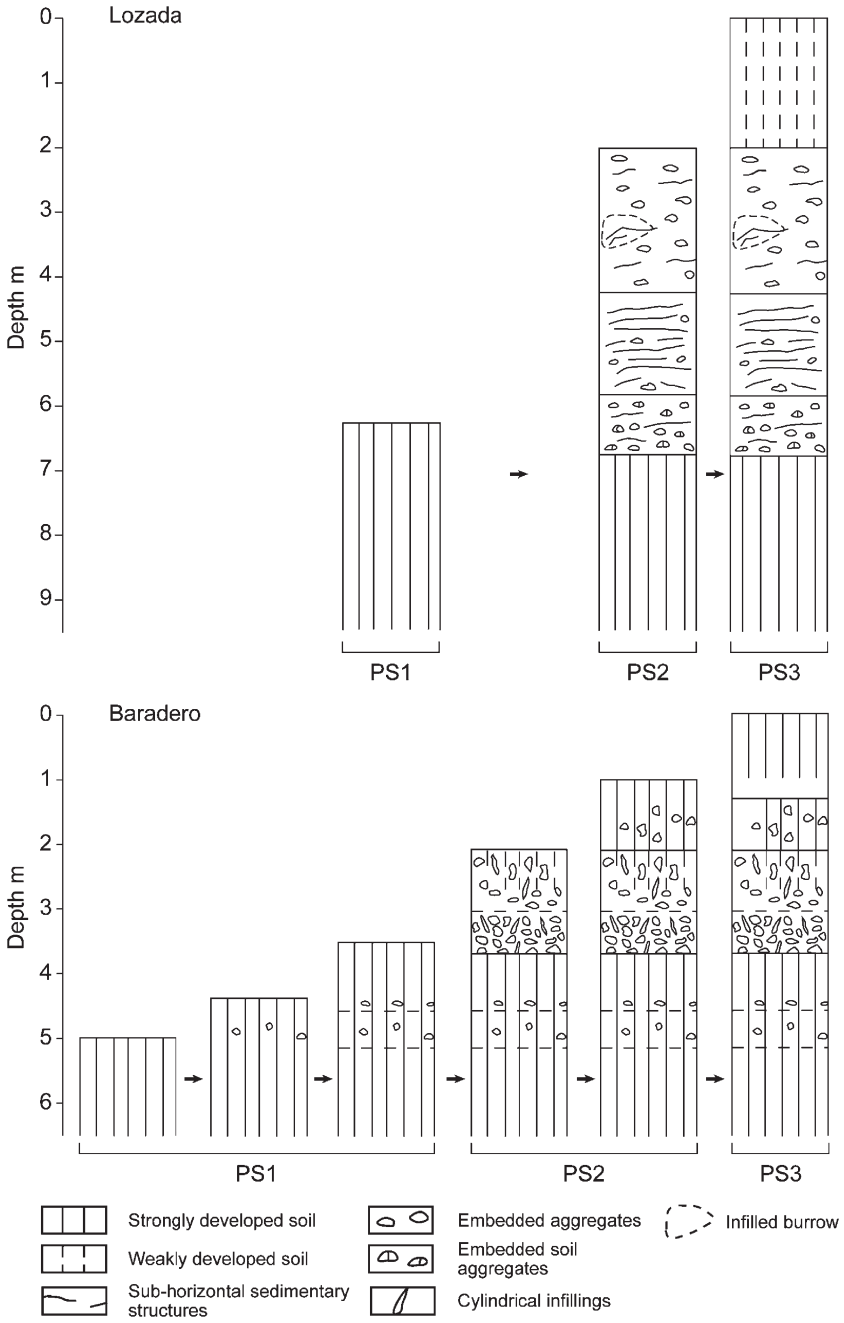

Figure 9. Reconstruction of the sequence of pedosedimentary stages (PS1–3) responsible for the development of the profiles at Lozada and Baradero. PS1 (prior to ca. 80,000 yr): Lozada, loess deposition and soil formation; Baradero, paludal sedimentation and soil formation (possibly more than one cycle separated by reworking and resulting in several sola welded to each other). PS2 (ca. 80,000 to 25,000 yr): Lozada, truncation and deposition of fluvial sediments; Baradero, truncation and deposition of paludal sediments and increasing proportions of loess with two significant depositional breaks when soils developed. PS3 (ca. 25,000 yr to present): Lozada, loess deposition until the mid-Holocene and soil formation; Baradero, truncation and deposition of loess until the early Holocene and soil formation.

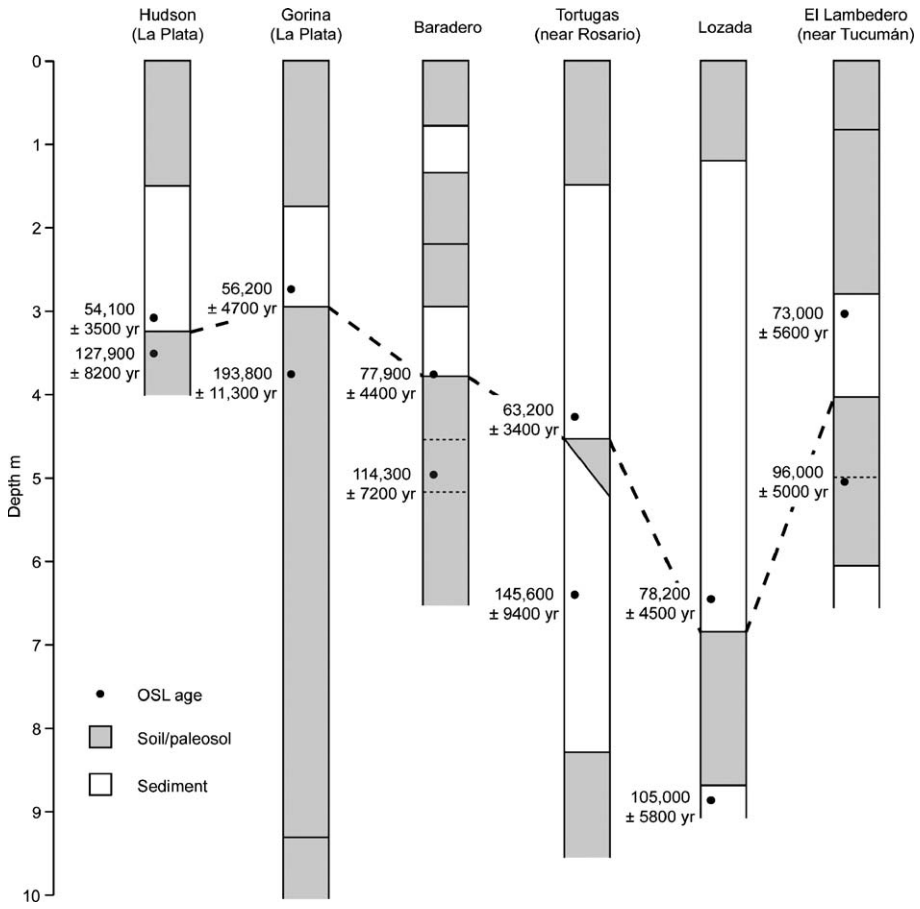

Figure 10. Tentative correlation of paleosols between sites near La Plata (Hudson, Gorina; Toms, unpublished data), Baradero, Rosario (Tortugas; Kemp et al., 2004a), Lozada and Tucuman (El Lambedero; Kemp et al., 2004b). Locations of these cities are shown in Figure 1. The soil stratigraphic unit is diachronous, probably spanning the equivalent of at least part of OIS 5.

deposition and several sola welded to each other. Although the paleosol (complex) at Baradero probably started forming before that at Lozada and therefore extended over a longer time period, it is still legitimate to correlate the two paleosols on the basis of the likely coincidence of pedogenic activity between ca. 105,000 (or possibly 90,000) and 80,000 yr. They therefore both probably developed during at least part of the last interglacial *sensu lato*, equivalent to oxygen isotope stage (OIS) 5 of the deep sea record (Martinson et al., 1987).

During pedosedimentary stage 2 at Baradero, between ca. 80,000 and 25,000 yr (OIS 4 and 3), there was a progressive change in depositional regime with eolian inputs gradually replacing paludal inputs. There were also two significant breaks in sedimentation when pedogenic activity dominated: the first resulted in a relatively weakly developed (ACk) profile and the second more intensive phase led to development of a Bt horizon, somewhat akin to that of the present surface soil. At Lozada, this whole pedosedimentary stage was characterized by fluvial activity with truncation of the paleosol and then deposition of sorted sediments, though bioturbation and carbonate redistribution processes were clearly active as the surface accreted.

Loess continued to accumulate at Baradero during the early part of pedosedimentary stage 3 until the early Holocene when the current land surface was established and the surface soil began to develop. This change is traditionally inferred to reflect a transition from relatively dry to more humid conditions brought about by a poleward shift of the Atlantic convergence zone with the dominant circulation from the northeast, or by a weakening of the South Atlantic anticyclone (Villagrán, 1993 in Prieto, 1996). The Lozada record, however, documents continued loess deposition well into the mid-Holocene, a delay reflecting the site's close proximity to source materials along the Andes piedmont in Mendoza Province. Here, the early Holocene remained relatively dry (D'Antoni, 1983; Zárate and Paez, 2002), thus encouraging continued eolian erosion from the Andean piedmont and transport of dust to Lozada at the western margin of the Pampas. The less developed nature of the surface soil at Lozada, particularly the lack of a Bt horizon, compared to that at Baradero thus reflects a combination of a drier climate and shorter soil-forming interval.

Conclusions

The Lozada and Baradero sections contain important records of landscape development during the late Quaternary in the Northern Pampa of Argentina. At Baradero, geomorphologically located in a swampy environment of the Pampa Ondulada (undulating Pampa) region, paludal sediments provided the

parent material for a soil that probably developed during a period corresponding to all or part of OIS 5. The equivalent soil at Lozada, 500 km to the west in the piedmont of the Sierras Pampeanas and probably formed in loess during the latter part of OIS 5, was truncated and buried beneath fluvial sediments during the time span of OIS 4 and 3. At Baradero, over this period, there was a progressive change in depositional regime with eolian gradually replacing paludal inputs: two paleosol units mark temporary breaks in sedimentation and dominance by pedogenic processes. OIS 2 at both sites was marked by significant loess accumulation with accretion continuing into the mid-Holocene only at Lozada.

Although these reconstructions cannot easily be fitted to the existing stratigraphic schemes of Cantú (1992), Kröhling (1999a) or Riggi et al. (1986), it is possible to link them to results obtained from other sites studied during the course of our regional project (Figs. 1 and 10). These studies have reinforced previous assertions (Teruggi, 1957; Imbellone and Teruggi, 1993; Zárate, 2003) that much of the Argentinian 'loess' is not primary or in situ, but rather a mixture of eolian and fluvially or colluvially-reworked material. Furthermore, few of the pedo-sedimentary records are continuous and erosional hiatuses are common. Nevertheless, though the present chronology is tentative and clearly requiring confirmation and further refinement, it appears that it is possible for the first time to recognize and trace across a range of sites in Argentina a diachronous soil stratigraphic unit that probably spans the equivalent of at least part of OIS 5 (Fig. 10). Although in some considerable way from establishing a stratigraphic framework of the quality and utility found in other loess areas of the world, this marks a very important step in defining and establishing a regional pedostratigraphy for this region of Argentina.

Acknowledgments

We would like to thank the Leverhulme Trust (grant F/07 537/A) for their financial support, James Smith and Alan Williams for some of the laboratory analysis, Jenny Kynaston for drawing the diagrams, and Art Bettis, Dan Muhs and Ashok Singhvi for their very helpful review comments.

References

Adamiec, G., Aitken, M.J., 1998. Dose-rate conversion factors: new data. Ancient TL 16, 37–50.

Antoine, P., Rousseau, D.D., Zöller, L., Lang, A., Munaut, A.V., Hatté, C., Fontugne, M., 2001. High-resolution record of the last Interglacial-glacial cycle in the Nussloch loess–palaeosol sequences, Upper Rhine Area, Germany. Quaternary International 76/77, 211–229.

Bateman, M.D., Frederick, C.D., Jaiswal, M.K., Singhvi, A.K., 2003. Investigations into the potential effects of pedoturbation on luminescence dating. Quaternary Science Reviews 22, 1169–1176.

Berger, G.W., 2003. Luminescence chronology of late Pleistocene loess–paleosol and tephra sequences near Fairbanks, Alaska. Quaternary Research 60, 70–83.

Berger, G.W., Mulhern, P.J., Huntley, D.J., 1980. Isolation of silt-sized quartz from sediments. Ancient TL 11, 147–152.

Bullock, P., Fedoroff, N., Jongerius, A., Stoops, G., Tursina, T., 1985. Handbook for Soil Thin Section Description. Waine Research, Wolverhampton.

Camilión, M., Mormeneo, L., Iñiguez, A., Maggi, J., 1992. Clay minerals and particle size distribution in the loessic sediments of the north-east Pampa Plain, Argentina. In: Derbyshire, E. (Ed.), Loess and the Argentine Pampa. Leicester University Geography Department Occasional Paper, pp. 24–29.

Cantú, M., 1992. El Holoceno de la Provincia de Córdoba. In: Iriondo, M. (Ed.), Primer Simposio Internacional del Holoceno. Entre Ríos, Paraná, pp. 1–16.

Carignano, C.A., 1999. Late Pleistocene to recent climate change in Córdoba Province Argentina: geomorphological evidence. Quaternary International 57/58, 117–134.

D'Antoni, H., 1983. Pollen analysis of Gratua del Indio. Quaternary of South America and Antarctic Peninsula 1, 83–104.

Galbraith, R.F., Roberts, R.G., Laslett, G.M., Yoshida, H., Olley, J.M., 1999. Optical dating of single and multiple grains of quartz from Jinmium rock shelter (northern Australia): Part I. Experimental design and statistical models. Archaeometry 41, 339–364.

Gale, S.J., Hoare, P.G., 1992. Quaternary Sediments: Petrographic Methods for the Study of Unlithified Rocks. Belhaven Press, London.

Goble, R.J., Mason, J.A., Loope, D.B., Swinehart, J.B., 2004. Optical and radiocarbon ages of stacked paleosols and dune sands in the Nebraska Sand Hills, USA. Quaternary Science Reviews 23, 1173–1182.

Grimley, D.A., Follmer, L.R., Hughes, R.E., Solheid, P.A., 2003. Modern, Sangamon and Yarmouth soil development in loess of unglaciated southwestern Illinois. Quaternary Science Reviews 22, 225–244.

INTA, 1989. Mapa de Suelos de la Provincial de Buenos Aires. Secretaria Agricultura Ganadería y Pesca. Programa Nacionales Unidas par el Desarrollo, Buenos Aires.

Imbellone, P.A., Teruggi, M.E., 1993. Paleosols in loess deposits of the Argentine Pampas. Quaternary International 17, 49–55.

Imbellone, P.E., Cumba, A., 2003. Una sucesión con paleosuelos superpuestos del Pleistoceno medio tardío-Holoceno, zona sur de la Plata, provincia de Buenos Aires. Revista de la Asociación Argentina de Sedimentología 10, 3–22.

Iriondo, M.H., 1997. Models of deposition of loess and loessoids in the Upper Quaternary of South America. Journal of South American Earth Sciences 10, 71–79.

Iriondo, M.H., 1999. Climatic changes in the South American plains: records of a continent-scale oscillation. Quaternary International 57–58, 93–112.

Jackson, M.L., Sayin, M., Clayton, R.N., 1976. Hexafluorosilicic acid reagent modification for quartz isolation. Soil Science Society of America Journal 40, 958–960.

Kemp, R.A., 2001. Pedogenic modification of loess: significance for palaeoclimatic reconstructions. Earth Science Reviews 54, 145–156.

Kemp, R.A., Derbyshire, E., Meng, X.M., 2001. A high-resolution micromorphological record of changing landscapes and climates on the western Loess Plateau of China during Oxygen Isotope Stage 5. Palaeogeography, Palaeoclimatology, Palaeoecology 170, 157–169.

Kemp, R.A., Toms, P.S., Sayago, J.M., Derbyshire, E., King, M., Wagoner, L., 2003. Micromorphology and OSL dating of the basal part of the loess–paleosol sequence at La Mesada in Tucumán province, Northwest Argentina. Quaternary International 106/107, 111–117.

Kemp, R.A., Toms, P.S., King, M., Kröhling, D.M., 2004a. The pedosedimentary evolution and chronology of Tortugas, a Late Quaternary type-site of the northern Pampa, Argentina. Quaternary International 114, 101–112.

Kemp, R.A., King, M., Toms, P., Derbyshire, E., Sayago, J.M., Collantes, M.M., 2004b. Pedosedimentary development of part of a Late Quaternary loess–palaeosol sequence in Northwest Argentina. Journal of Quaternary Science 19, 567–576.

Kröhling, D.M., 1999a. Upper Quaternary geology of the lower Carcarañá Basin, North Pampa, Argentina. Quaternary International 57/58, 135–148.

Kröhling, D.M., 1999b. Sedimentological maps of the typical loessic units in North Pampa, Argentina. Quaternary International 62, 49–55.

Lee, J.A., Kemp, R.A., 1992. Thin Sections of Unconsolidated Sediments and Soils: a Recipe. Centre for Environmental Analysis and Management Technical Report, Department of Geography, Royal Holloway, University of London.

Martinson, D.G., Pisias, N.G., Hays, J.D., Imbrie, J., Moore, T.C., Shackleton, N.J., 1987. Age dating and the orbital theory of the ice ages: development of a high-resolution 0 to 300,000-year chronostratigraphy. Quaternary Research 27, 1–29.

McDonald, E.V., Busacca, A.J., 1990. Interaction between aggrading geomorphic surfaces and the formation of a Late Pleistocene paleosol in the Palouse loess of eastern Washington state. Geomorphology 3, 449–470.

Mestdagh, H., Haesarts, P., Dodonov, A., Hus, J., 1999. Pedosedimentary and climatic reconstruction of the last interglacial and early glacial loess–paleosol sequence in South Tadzhikistan. Catena 35, 197–218.

Mücher, H.J., Vreeken, W.J., 1981. (Re)deposition of loess in Southern Limbourg, the Netherlands. 2. Micromorphology of the Lower Silt Loam Complex and comparison with deposits produced under laboratory conditions. Earth Surface Processes and Landforms 6, 355–363.

Muhs, D.R., Zárate, M., 2001. Late Quaternary eolian records of the Americas and their paleoclimatic significance. In: Markgraf, V. (Ed.), Interhemispheric Climate Linkages. Academic Press, San Diego, pp. 183–226.

Muhs, D.R., Bettis III, E.A., Been, J., McGeehin, J.P., 2001. Impact of climate and parent material on chemical weathering in loess-derived soils of the Mississippi River Valley. Soil Science Society of America Journal 65, 1761–1777.

Muhs, D.R., Ager, T.A., Bettis III, E.A., McGeehin, J., Been, J.M., Begét, J.E., Pavich, M.J., Stafford Jr., T.W., Stevens, D.A.S.P., 2003. Stratigraphy and paleoclimatic significance of Late Quaternary loess–paleosol sequences of the Last Interglacial–Glacial cycle in central Alaska. Quaternary Science Reviews 22, 1947–1986.

Murray, A.S., Funder, S., 2003. Optically stimulated luminescence dating of a Danish Eemian coastal marine deposit: a test of accuracy. Quaternary Science Reviews 22, 1177–1183.

Murray, A.S., Wintle, A.G., Wallinga, J., 2002. Dose estimation using quartz OSL in the non-linear region of the growth curve. Radiation Protection Dosimetry 101, 371–374.

Nabel, P.E., Camilión, M.C., Machado, G.A., Spiegelman, A., Mormeneo, L., 1993. Magneto y litoestrafigrafía de los sedimentos pampeanos en los alrededores de la ciudad de Baradero, Provincia de Buenos Aires. Revista de la Asociación Geológica Argentina 48, 193–206.

Olley, J.M., Pietsch, T., Roberts, R.G., 2004. Optical dating of Holocene sediments from a variety of geomorphic settings using single grains of quartz. Geomorphology 70, 337–358.

Prescott, J.R., Hutton, J.T., 1994. Cosmic ray contributions to dose rates for luminescence and ESR dating: large depths and long-term time variations. Radiation Measurements 23, 497–500.

Prieto, A., 1996. Late Quaternary vegetational and climatic changes in the Pampa grassland of Argentina. Quaternary Research 45, 73–88.

Reineck, H.E., Singh, I.B., 1980. Depositional Sedimentary Environments. Springer-Verlag, New York.

Riggi, J.C., Fidalgo, F., Martinez, O., Porro, N., 1986. Geología de los sedimentos pampeanos en el área de la Plata. Revista de la Asociación Geológica Argentina 316–333.

Sanabria, J., Arguello, G., 1999. La edad de los materiales parentales loéssicos de los suelos y desarrollo del perfil, en un sector de la plataforma basculada, Córdoba, Argentina. Resúmenes de XI Congreso Latinoamericano de la Ciencia del Suelo, Temuco, Chile, pp. 210–214.

Schellenberger, A., Heller, F., Veit, H., 2003. Magnetostratigraphy and magnetic susceptibility of Las Carreras loess–paleosol sequence in Valle de Tafí, Tucumán, NW Argentina. Quaternary International 106/107, 159–167.

Singhvi, A.K., Bluszcz, A., Bateman, M.D., Someshwar Rao, M., 2001. Luminescence dating of loess–palaeosol sequences and coversands: methodological aspects and palaeoclimatic implications. Earth Science Reviews 54, 193–211.

Soil Survey Staff, 1992. Keys to Soil Taxonomy. Soil Management Support Services Technical Monograph, vol. 19. Pocahontas Press, Blacksburg, VA.

Teruggi, M.E., 1957. The nature and origin of Argentine loess. Journal of Sedimentary Petrology 27, 322–332.

Toms, P.S., King, M., Zárate, M.A., Kemp, R.A., Foit Jr., F.F., 2004. Geochemical characterization, correlation and optical dating of tephra in alluvial sequences of central western Argentina. Quaternary Research 62, 60–75.

Tonni, E.P., Nabel, P., Cione, A.L., Etchichury, M., Tófalo, R., Scillato Yané, G., San Cristóbal, J., Carlini, A., Vargas, D., 1999. The Ensenada and Buenos Aires formations (Pleistocene) in a quarry near La Plata, Argentina. Journal of South American Earth Sciences 12, 273–291.

Zárate, M., 2003. Loess of southern South America. Quaternary Science Reviews 22, 1997–2006.

Zárate, M., Paez, M., 2002. Los paleoambientes del Pleistoceno-Holoceno en la cuenca del arroyo La Estacada, Mendoza. In: Trombotto, D., Villalba, R. (Eds.), 30 Años de Investigación Básica y Aplicada en Ciencias Ambientales. Instituto de Nivología, Glaciología y Ciencias Ambientales, Mendoza, pp. 117–122.

Zimmerman, D.W., 1971. Thermoluminescence dating using fine grains from pottery. Archaeometry 13, 29–52.

Zinck, J.A., Sayago, J.M., 1999. Loess–paleosol sequence of La Mesada in Tucumán province, northwest Argentina: characterization and paleoenvironmental interpretation. Journal of South American Earth Sciences 12, 293–310.

Zinck, J.A., Sayago, J.M., 2001. Climatic periodicity during the late Pleistocene from a loess–paleosol sequence in northwest Argentina. Quaternary International 78, 11–16.